(n,α) cross section measurement of light nuclei using gridded ionization chamber and gaseous sample

Toshiya Sanami, Mamoru Baba, Keiichiro Saito, Yasutaka Ibara*,
Tetsuro Yamazaki, Jun Sato, Naohiro Hirakawa
Quantum Science and Energy Engineering, Tohoku University, Sendai 980-77

e-mail : toshi@rpl.qse.tohoku.ac.jp, mamoru.baba@qse.tohoku.ac.jp

We have developed a measuring method of (n,α) cross section by using gaseous sample in a gidded ionization chamber. In this study, we measured the $^{12}C(n,\alpha_0)$ and the $^{16}O(n,\alpha_0)$, (n,α_{123}) cross sections for En=11.5 and 12.8 MeV neutrons. We also deduced the $^{12}C(n,x\alpha)$ spectrum and analyzed the data by a kinematic calculation combined with the reaction data of the $^{12}C(n,n'3\alpha)$.

1. Introduction

Neutron induced α production cross section data of light nuclei are required in various fields, i.e, nuclear engineering, biological and medical fields. In spite of the importance of the data, there are few experimental data, even for C, O and N, in En=10-20 MeV region, probably because of experimental difficulty and the unavailability of an appropriate foil sample of ^{16}O and ^{14}N. In addition, theoretical calculations are ambiguous in estimation of the cross section. This condition causes large uncertainty in experimental data and evaluations.

We have conducted the measurements of $(n,x\alpha)$ cross sections of Fe, Ni, Cr and Cu by a gridded ionization chamber (GIC) and foil samples **[1,2]**. Recently, we have extended the measurements to light nuclei by using gaseous samples. This method enables cross section measurements in a very large solid angle without distortion by the energy loss in samples, but requires a method to estimate the effective number of sample atoms and the magnitude of the wall effects **[3]**. We found the method to eliminate the effects by using GIC signals and a tight neutron collimation. In this study, we describe the recent results of the $^{12}C(n,\alpha_0)$ and the $^{16}O(n,\alpha_0)$, (n,α_{123}) cross sections for 11.5 and 12.8 MeV neutrons. We also present the analysis of the $^{12}C(n,x\alpha)$ spectrum for 14.1 MeV neutrons to estimate the $^{12}C(n,n'3\alpha)$ reaction process.

2. Experimental method

The experiments were carried out at Tohoku University 4.5MV Dynamitoron accelerator laboratory.

* Present address : Kandenko co.,ltd.

Experimental method is same as in the former experiments in Ref. 3. Neutrons of 11.5 and 12.8 MeV were produced via the $^{15}N(d,n)^{16}O$ reaction in a $^{15}N_2$ gas target. The neutrons are quasi mono-energetic, but the 11.5 and 12.8 MeV neutrons are apart about 6 MeV from contaminate neutrons feeding to the excited states of residual nuclei ^{16}O **[4]**. Therefore, we can treat the source neutron to be monoenergy for the $^{12}C(n,\alpha)$ and the $^{16}O(n,\alpha_0)$, (n,α_{123}) reactions with high threshold energy. The neutrons were collimated with a 15 cm long Cu collimator to irradiate sample gases contained in a counting gas of GIC. The counting gas is $Kr+CH_4$ and $Kr+CO_2$ mixtures to measure the $^{12}C(n,x\alpha)$ and $^{16}O(n,x\alpha)$, respectively. Alpha particles from the sample gas ionize the counting gas and produce two output signals, Pa and Pc (anode and cathode, respectively). If alpha particles are produced and stopped between the cathode and the grid electrode, Pa and Pc are represented by the following equations,

$$Pa=Ca\cdot(E+\sigma Pc) \quad \text{and} \quad Pc=Cc\cdot E(1-x/d), \qquad (1),(2)$$

where, Ca and Cc are the amplitude factor of the anode and the cathode, respectively, E is the particle energy, σ is the grid inefficiency (5.9%), x is the distance between the cathode plate and the center-of-gravity of electrons (detection position). By choosing an appropriate gas pressure and combining Pa and Pc, we can find the detection position (x) of each event to pick up the events that give full energies to GIC.

$$x=d\cdot(1-Ca\cdot Pc/(Ca\cdot Pa+\sigma\cdot Ca\cdot Cc\cdot Pc)) \qquad (3)$$

By this method and the tight neutron collimation, we can determine the number of sample atoms irradiated by neutrons.

The running time was about 3 and 9 hours with 4μA beam current of D^+ ion for 11.5 and 12.8 MeV measurement, respectively. Alpha yields in a central volume of GIC were selected by using the anode and the cathode signals according to eq.3. The number of sample atoms was determined from the neutron beam profile and the volume of the sample region. The neutron profile was measured with an imaging plate **[5]**, and the neutron flux was measured with a recoil-proton counter telescope **[6]**.

3. Data reduction and error estimation

Fig. 1 shows a two-dimensional spectrum of the 3.0 kgf/cm^2 $Kr+CH_4$ gas for 14.1MeV neutrons. The events from the $^{12}C(n,\alpha_0)^9Be$ reaction forms the vertical strip because the anode signal shows sum energy of the α_0 and the ^9Be particle. The $^{12}C(n,n'3\alpha)$ events show continuous distribution because neutrons do not deposite an energy in GIC. The background events from H(n,p) and Kr(n,α) were also observed, but H(n,p) events exist only in the low energy region and Kr(n,α) events are negligibly few. Cross sections were deduced by

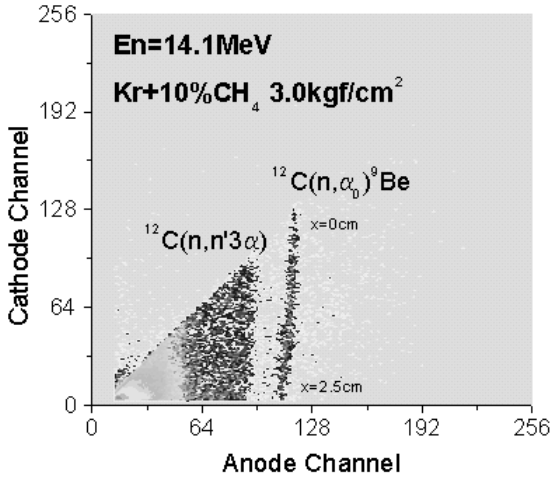

Fig. 1 Two dimensional spectrum of $Kr+10\%CH_4$

the relation,

$$Y=N\cdot\sigma\cdot\phi\,, \qquad (4)$$

where Y is the yield in the center of GIC, N is the number of sample atom, σ is the reaction cross section, ϕ is the neutron flux measured by counter telescope. For the $^{12}C(n,\alpha_0)$ reaction, Y is obtained from the peak yield of the $Kr+CH_4$ spectrum. In the case of the $^{16}O(n,\alpha)$, it is obtained from the difference between the spectra for $Kr+CH_4$ and $Kr+CO_2$ **[3]**. We estimate errors from the counting statistics, the effective area and the normalization by the neutron flux. The total error is about 12% in the worst case.

4. Results and discussion

4-1.The $^{12}C(n,\alpha_0)$ cross sections

Fig. 2 shows the $^{12}C(n,\alpha_0)$ cross sections in comparison with other experimental results **[7]** and evaluations. There is no other experimental $^{12}C(n,\alpha_0)$ data around 12 MeV, but our data are consistent with evaluations and connects smoothly between the results in low and high energy. As shown later, the $^{12}C(n,\alpha_0)$ reaction is not a dominant process of the $^{12}C(n,x\alpha)$ above 10 MeV region. Therefore, the $^{12}C(n,n'3\alpha)$ process is important for the $^{12}C(n,x\alpha)$ cross section in this region.

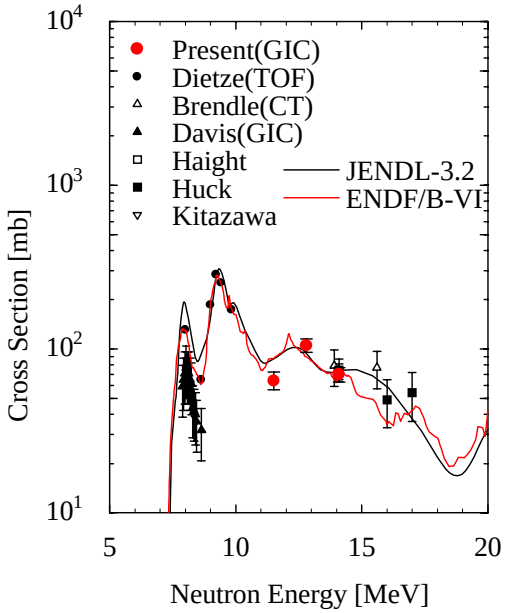

Fig. 2 $^{12}C(n,\alpha_0)$ cross sections

4-2. $^{12}C(n,n'3\alpha)$ spectrum

The $^{12}C(n,n'3\alpha)$ reaction has many reaction process **[10][11]**. In this study, we deduce a total energy spectrum of the $^{12}C(n,x\alpha)$ reaction and compare with a simple calculation. Figure 3 shows the energy spectrum of $Kr+CH_4$ gas for 14.1 MeV neutrons at various counting gas pressure. From high-pressure result, the $^{12}C(n,\alpha_0)$ peak and the $^{12}C(n,n'3\alpha)$ edge could be observed clearly, but low energy α events are hidden by protons form H(n,p) reaction. On the other hand, the peak and the edge disappear in the low-pressure result, but details of structures in low energy region can still be observed. Therefore, by the combining these two results, we can obtain the energy spectrum with little proton contamination. This spectrum also contains the recoil

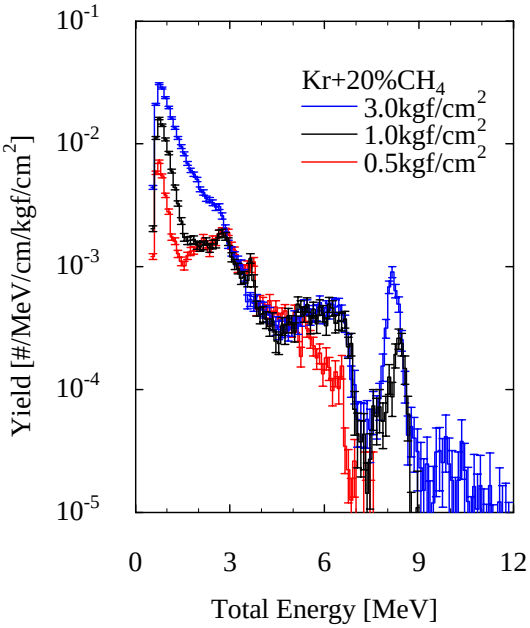

Fig. 3 $Kr+CH_4$ spectrum in various pressures

particles from the $^{12}C(n,n')^{12}C$ reaction.

To simulate the spectrum, we calculate the contributions of each reaction. The recoil ^{12}C from $^{12}C(n,n_{el})$ and $^{12}C(n,n_1)$ reaction, and α_0 energy spectrum are obtained by the kinematics calculation using the cross section data by JENDL-3.2 with the Gaussian smearing (0.5 MeV FWHM). About the $^{12}C(n,n'3\alpha)$ channel, dominant channels are as follows **[10,11]**.

(1) 2body + 3 body simultaneous decay : $^{12}C(n,n')\,^{12}C^*_{Ex}$, $^{12}C^*_{Ex} \rightarrow 3\alpha$

(2) 2body + 3body simultaneous decay : $^{12}C(n,\alpha)\,^{9}Be_{Ex}$, $^{9}Be_{Ex} \rightarrow 2\alpha+n$

(3) 3body + 2body sequential decay : $^{12}C(n,n'\alpha)^{8}Be$, $^{8}Be \rightarrow 2\alpha$

The sum energy of 3α, $E_{3\alpha}$, is the calculated by following equation,

$$E_{3\alpha}=E_{in}+Q_{(n,n'3\alpha)}-E_n\,,$$

where, E_{in} is the incident neutron energy, $Q_{(n,n'3\alpha)}$ is the Q-value of the $^{12}C(n,n'3\alpha)$ reaction and E_n is the ejected neutron energy. The calculation for process (1) was done by 2-body kinematics using the (n,n') data in JENDL-3.2. The 3-body simultaneous decay (2) and (3) was calculated based on a 3-body phase space model **[8]**,

$$d\sigma/dE=C_0^2\cdot(E_{cm}\cdot(E_{max}-E_{cm}))^{1/2}\,, \qquad (4)$$

where, $d\sigma/dE$ is the energy spectrum of the center-of-mass system and E_{max} is the maximum kinematically allowed energy of the ejectile particle. The relationship of the two sequential process was considered by an analytical method **[9]**.

Fig. 4 and 5 shows the comparison between experimental results and calculation using the branching ratio in Refs. 9 and 10, respectively. In figure 4, the calculation considering the process (1) [only for Ex=9.63 MeV state] and (3) underestimates the high energy edge of the $^{12}C(n,n'3\alpha)$ reaction. In contrast, in Fig. 5, the calculation taking account of (1) [Ex is 7.66, 9.63, 10.1, 10.8, 11.1, 12.7 MeV] and (2) [Ex=2.43MeV] processes, are in fair agreement with the experiment around the edge. In the low energy part, the experimental data would still contain the proton contaminant by H(n,p).

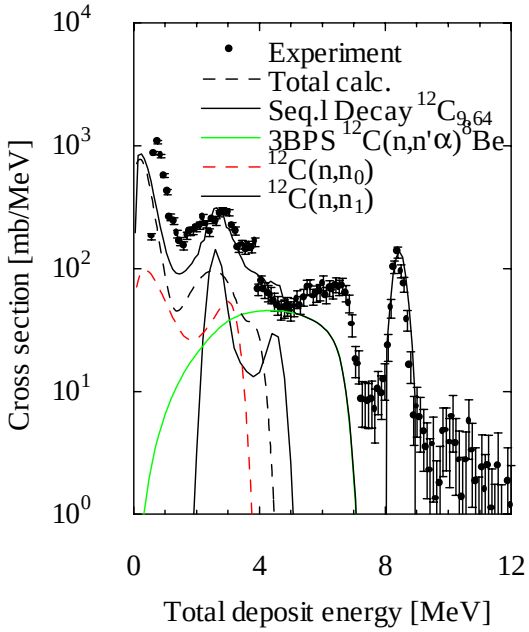

Fig. 4 $^{12}C(n,x\alpha)$ spectrum with calculation **[9]**

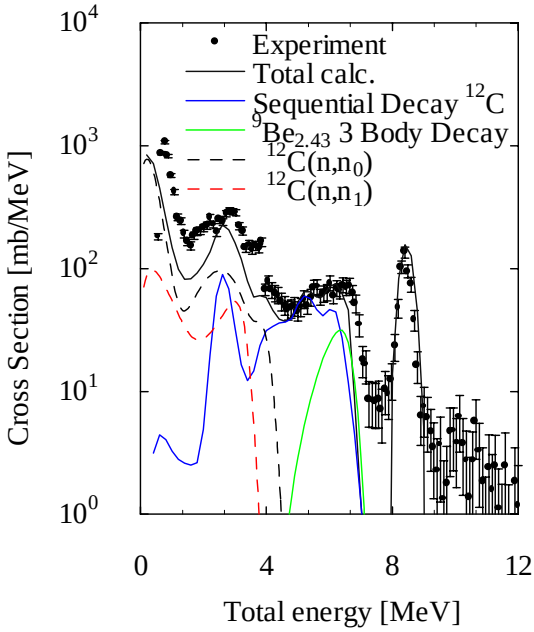

Fig. 5 $^{12}C(n,x\alpha)$ spectrum with calculation **[10]**

4-3. $^{16}O(n,\alpha)$ cross section

Fig. 6 and 7 show the $^{16}O(n,\alpha_0)$ and the $^{16}O(n,\alpha_{1,2,3})$ cross sections together with evaluations and other experimental results **[12-16]** by γ-detection and the counter telescope method. In Fig. 6, the present results are in fair agreement with others, but, about the $^{16}O(n,\alpha_{1,2,3})$ cross sections, there is some difference between present and orphan data.

Fig. 8 shows the result of the $^{16}O(n,x\alpha)$ cross section in comparison with the evaluations and other experimental results **[16-18]** by the emulsion, cloud chamber and scintillator method. In the case of ENDF/B-VI, the $^{16}O(n,x\alpha)$ cross section is given by the sum of the $^{16}O(n,\alpha_0)$, the $^{16}O(n,\alpha_{1,2,3})$ and some neutron inelastic scattering cross section. In the case of JENDL-3.2, the cross section is given by the sum of the $^{16}O(n,\alpha)$ and the $^{16}O(n,n'\alpha)$. In comparison between experimental data, the present value at 14.1 and 15.0 MeV are slightly smaller. The reason is that the $^{16}O(n,n'\alpha)$ cross section was obtained by summing the α events with channel energy below 4 MeV. Then, our values do not include the α events with low channel energy and might result in underestimation of the cross section.

From these results, the difference between the experimental values and JENDL can not be explained only by the difference in the $^{16}O(n,\alpha_0)$ and the $^{16}O(n,\alpha_{123})$ branch. Therefore, we can conclude that the key of the $^{16}O(n,x\alpha)$ cross section determination is the $^{16}O(n,n'\alpha)$ value.

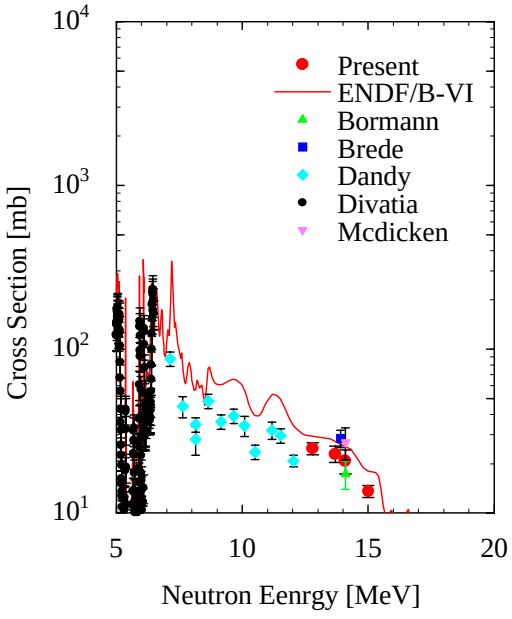

Fig. 6 $^{16}O(n,\alpha_0)$ cross sections

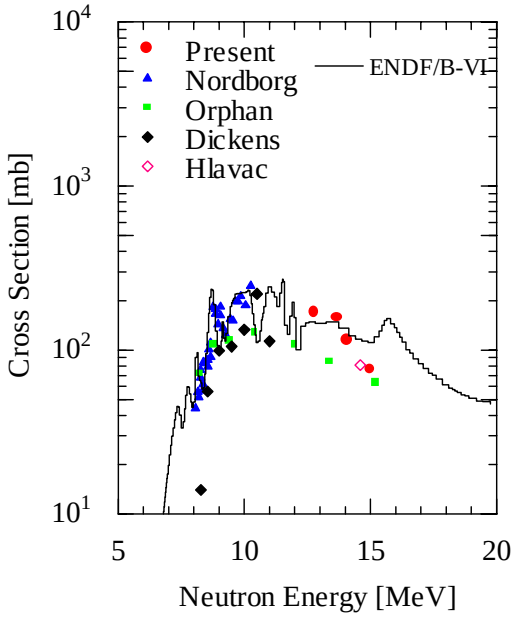

Fig. 7 $^{16}O(n,\alpha_{1,2,3})$ cross sections

5. Conclusion

In this study, we described the results of the $^{12}C(n,\alpha_0)$ and the $^{16}O(n,\alpha_0)$, (n,α_{123}) cross section for En=11.5

and 12.8 MeV by a measuring method using gaseous sample and GIC, and the analysis of $^{12}C(n,n'3\alpha)$ reaction. We should note that the method is useful for light nuclei cross section measurement.

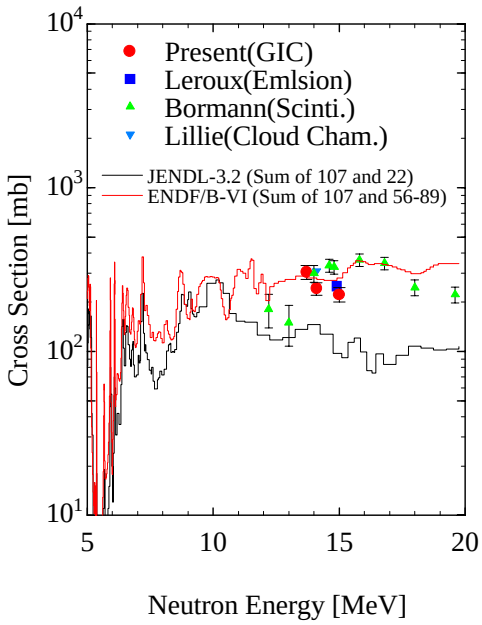

Fig. 8 $^{16}O(n,\alpha)$ cross sections

References

1. N.Ito, M.Baba, S.Matsuyama, I.Matsuyama and N.Hirakawa, *Nucle.Instrm. Methods*, **A337**, 474 (1994)
2. M.Baba, N.Ito, I.Matsuyama, S.Matsuyama, N.Hirakwa, S.Chiba, T.Fukahori, M.Mizumoto, Kazuo.Hasegawa and S.Meigo, *J.Nucl.Sci.Technol*., **31**, 745 (1994)
3. T.Sanami, M.Baba, K.Saito, Y.Ibara and N.Hirakawa, *Proc.Int.Conf. on nucle Data for Sci. and Technol*. (Trieste, Italy 1997), to be published
4. J.L.Weil and K.W.Jones, *Phys.Rev.*, **112** 1775 (1985)
5. T. Sanami, M.Baba, K.Saito, Y.Ibara, A.Yamadera, S.Taniguchi, T.Nakamura and N.Hirakawa, *Proc. of 10th workshop on radiation detectors and their uses*, (KEK, Tukuba, 1997), p74
6. M.Baba, M.Takada, T.Iwasaki, S.Matsuyama, T.Nakamura, H.Ohguchi, T.Nakao, T.Sanami and N.Hirakawa, *Nucle.Instrm.Meth*., **A376**, 115 (1996)
7. R.C.Haight, S.M.Grims, R.G.Johnson and H.H.Barschall, *Nucl.Sci.Eng.* **87**, 41 (1984)
8. G.G.Olsen, *Nucl.Instrm.Meth*., **37**, 240 (1965)
9. M.D.Baker, H.D.Knox and E.reitenberger, *Nucl.Sci.Eng*., **96**, 39 (1987)
10. B.Antolkovic, I.Slaus, D.Plenkovic, P.Maco and J.P.Meulders, *Nucl.Phys*., **A394**, 87 (1983)
11. B.Antolkovic, G.Dietze and H.Klein, *Nucl.Sci.Eng*., **107**, 1 (1991)
12. C.Nordborg and L.Nilsson: ,*Nucl.Sci.Eng.*, **66**, 75 (1978)
13. V.J.Orphan, C.G.Hoot and Joseph John, *Nucl.Sci.Eng.*, **42**, 352 (1970)
14. J.K.Dickens and F.G.Perey : *Nucl.Sci.Eng.*, **40**, 283 (1970)
15. S.Hlavac, P. Oblozinsky, I. Turzo, L. Dostal and J. Kliman, private communication
16. B.Leroux, K.El-Hammami, J.Dalmas, R.Chastel, G.Lamot, C.Fayard and J.H.Boutros: *Nucl.Phys* **A116**, 196 (1968)
17. M.Bormann, S.Cierjacks, E.Fretwurst, K.-J.Giesecke, H.Neuert and H.Pollehn:*Z.Phys* **174**, 1 (1963)
18. A.B.Lillie, *Phys.Rev*. **87,** 716 (1952)